

Static and dynamic instability analyses of 1400-meter long-span cable-stayed bridges

Autor(en): **Nagai, Masatsugu / Xie, Xu / Yamaguchi, Hiroki**

Objekttyp: **Article**

Zeitschrift: **IABSE reports = Rapports AIPC = IVBH Berichte**

Band (Jahr): **79 (1998)**

PDF erstellt am: **27.06.2024**

Persistenter Link: <https://doi.org/10.5169/seals-59874>

Nutzungsbedingungen

Die ETH-Bibliothek ist Anbieterin der digitalisierten Zeitschriften. Sie besitzt keine Urheberrechte an den Inhalten der Zeitschriften. Die Rechte liegen in der Regel bei den Herausgebern.

Die auf der Plattform e-periodica veröffentlichten Dokumente stehen für nicht-kommerzielle Zwecke in Lehre und Forschung sowie für die private Nutzung frei zur Verfügung. Einzelne Dateien oder Ausdrucke aus diesem Angebot können zusammen mit diesen Nutzungsbedingungen und den korrekten Herkunftsbezeichnungen weitergegeben werden.

Das Veröffentlichen von Bildern in Print- und Online-Publikationen ist nur mit vorheriger Genehmigung der Rechteinhaber erlaubt. Die systematische Speicherung von Teilen des elektronischen Angebots auf anderen Servern bedarf ebenfalls des schriftlichen Einverständnisses der Rechteinhaber.

Haftungsausschluss

Alle Angaben erfolgen ohne Gewähr für Vollständigkeit oder Richtigkeit. Es wird keine Haftung übernommen für Schäden durch die Verwendung von Informationen aus diesem Online-Angebot oder durch das Fehlen von Informationen. Dies gilt auch für Inhalte Dritter, die über dieses Angebot zugänglich sind.



Static and Dynamic Instability Analyses of 1400-meter Long-Span Cable-Stayed Bridges

Masatsugu NAGAI
Prof.
Nagaoka Univ. of Technology
Nagaoka, Japan

Xu XIE
Research Assoc.
Saitama Univ.
Urawa, Japan

Hiroki YAMAGUCHI
Prof.
Saitama Univ.
Urawa, Japan

Yozo FUJINO
Prof.
Univ. of Tokyo
Tokyo, Japan

Summary

This paper describes static and dynamic instability analyses of long-span cable-stayed bridges. They are elasto-plastic finite displacement analysis under in-plane load, finite displacement analysis under displacement-dependent wind load and flutter analysis. Using a 1400-meter cable-stayed bridge model, in which four types of cross-sectional shapes of the girder are selected, static and dynamic instability analyses are carried out. Finally, the design materials for identifying a minimum cross sectional shape of the girder, which ensures safety against above instabilities, are presented.

1. Introduction

In the design of long-span cable-stayed bridges, ensuring safety against static and dynamic instabilities is an important issue, because the shape and dimension of the girder are controlled by the above instabilities. However, static and dynamic instability phenomena of long-span cable-stayed bridges based on analytical procedures have not been made clear so far. In this paper, using a 1400-meter cable-stayed bridge model, static and dynamic instability analyses such as elasto-plastic finite displacement analysis under in-plane load, finite displacement analysis under displacement-dependent wind load and flutter analysis based on modal coordinate are carried out. Four types of cross section of the box girder are chosen. The span/width ratio is 56 and 47, and the span/depth ratio is 400 and 350, respectively. It is recommended, for ensuring safety against out-of-plane instability under wind load, that the span/width ratio should be less than 40. However, in this study, the larger values are employed. The employed cross sections are preliminary designed, in which the yield point of the material only is selected to be instability criterion. By carrying out the above instability analyses, the factor of safety under in-plane load, critical wind velocity of lateral torsional buckling and flutter onset wind velocity are presented. Finally, the design materials for obtaining minimum cross-sectional shape and dimension of the girder is presented



2. Analytical procedure

2.1 Elasto-plastic finite displacement analysis under vertical load ¹⁾

For evaluating load carrying capacity of the cable-stayed bridges, not only geometrical but also material nonlinear behaviors should be taken into account. The fundamental equation of elasto-plastic finite displacement analysis is given by

$$([K_{ep}] + [K_{\sigma}])\{\Delta u\}^e = \{\Delta f\}^e \quad (1)$$

$$[K_{ep}] = \int_v [B]^T [D_{ep}] [B] dv \quad (2)$$

$$[K_{\sigma}] = \int_v [G]^T [\sigma] [G] dv \quad (3)$$

where, $[K_{ep}]$ and $[K_{\sigma}]$ are elasto-plastic and initial stress matrices, $\{\Delta u\}^e$ and $\{\Delta f\}^e$ are incremental displacement and force vectors of the element, $[B]$ and $[G]$ are matrices consisted of interpolation functions, $[D_{ep}]$ is matrix relating to the constitutive law, $[\sigma]$ is matrix consisted of initial stress resultants.

In this formulation, the constitutive law of elastic perfect-plastic material is derived based on the Prandtl-Reuss equation. The yield condition is given by

$$\sqrt{\sigma^2 + 3\tau^2} - \sigma_y = 0 \quad (4)$$

Where, σ_y is the yield point of the material.

2.2 Finite displacement analysis under wind load ²⁾

In this analysis, the girder is subjected to the following three components of wind load, such as the drag force (D), lift force (L) and aerodynamic moment (M), which are given by

$$D(\alpha) = 0.5 \rho U_z^2 A_n C_D(\alpha)$$

$$L(\alpha) = 0.5 \rho U_z^2 B C_L(\alpha) \quad (5)$$

$$M(\alpha) = 0.5 \rho U_z^2 B^2 C_M(\alpha)$$

where, ρ is the air density, A_n is the vertical projection of the girder, B is the total width of the girder and C_D , C_L and C_M are aerodynamic coefficients.

U_z is the design wind velocity at the height of z , and is given by

$$U_z = (z/10)^{1/7} U_{10} \quad (6)$$

Where, U_{10} is the wind velocity at the height of 10 meters.

When the girder is subjected to the wind load, it displaces in the lateral direction and, at some wind velocity, it starts rotating. Due to the rotation of the girder, three components of aerodynamic forces above defined change, because they are dependent on an angle of attack (α) of the wind. This phenomenon should be taken into account³⁾. In this analysis, 4-node isoparametric cable element is used, thus the wind load acting on the cable is taken into account. In addition, the change of the tension in cables and its direction is considered. With respect to aerodynamic coefficients, the values of the Meiko-chuo bridge (590-meter cable-stayed bridge)³⁾ which were obtained from wind tunnel test, are used.

2.3 Flutter analysis based on modal coordinate⁴⁾

A fundamental equation of flutter analysis is derived based on modal coordinate and the effect of the cable local vibration on flutter onset wind velocity is taken into account. The unsteady drag

force of the girder is derived based on quasi-steady state theory, and the unsteady lift and aerodynamic moment are derived based on flat plate theory. The unsteady drag and lift forces of the cables are derived based on quasi-steady state theory.

The following is the fundamental equation of flutter analysis, which is expressed using both physical and modal coordinates.

$$[(M_{BC} - F_R) - iF_I] \begin{Bmatrix} \ddot{d} \\ \ddot{q}_C \end{Bmatrix} + [K_{BC}] \begin{Bmatrix} d \\ q_C \end{Bmatrix} = \{0\} \quad (7)$$

where, $\{d\}$ is the displacement of the girder and towers, $\{q_C\}$ is the generalized displacement of the cables, which corresponds to the cable local vibration, $[M_{BC}]$ and $[K_{BC}]$ are mass and stiffness matrices, respectively and $[F_R]$ and $[F_I]$ are real and imaginary parts of unsteady aerodynamic forces.

Carrying out eigenvalue analysis of the whole structure, in which cable local vibration is neglected, we obtain the modal matrix $[\phi]$. Using this matrix, eq.(10) is transformed into eq.(11). Where, $\{q\}$ is the generalized displacement, which corresponds to the global vibration.

$$[\phi]^T [(M_{BC} - F_R) - iF_I] [\phi] \begin{Bmatrix} \ddot{q} \\ \ddot{q}_C \end{Bmatrix} + [\phi]^T [K_{BC}] [\phi] \begin{Bmatrix} q \\ q_C \end{Bmatrix} = \{0\} \quad (8)$$

Assuming the reduced frequency, complex eigenvalue analysis is carried out, then we obtain complex eigenvalue of $\lambda = \lambda_R \pm i\lambda_I$. When the sign of the damping ($\xi = \lambda_R / \sqrt{\lambda_R^2 + \lambda_I^2}$) changes from plus to minus, flutter occurs.

3. BRIDGE MODEL

Fig.1(a) shows a side-view of a cable-stayed bridge model. Center and side spans are 1400 and 680 meters, respectively. In the side span, three intermediate piers are installed at a distance of 100 meters in order to increase in-plane flexural rigidity. Fig.1(b) is a front view of the tower, and the height of it from the deck level is one fifth of the center span length. Fig.1(c) shows the cross sectional shape of the girder. Four types of cross sections are used. In the Fig., B_u of 25 and 30 meters and h_w of 3.5 and 4.0 meters are selected. When calculating the stress from wind load, the design wind velocities of the girder and cables are assumed to be 60 and 70m/s, respectively. Those of them at the stage of erection are 70% of the above values. The drag coefficient (C_D) of them are assumed to be 0.8 and 0.7, respectively.

Dimension of the girder is determined by using the following criteria

$$\sigma_D + \sigma_L < \sigma_y / \gamma_1 \quad (\gamma_1 = 1.7) \quad (13)$$

$$\sigma_D + \sigma_w < \sigma_y / \gamma_2 \quad (\gamma_2 = 1.15) \quad (14)$$

where, σ_D , σ_L and σ_w are stresses from dead, live and wind loads, respectively, σ_y ($= 451\text{MPa}$) is the yield point of the employed material and γ is the factor of safety.

To satisfy eq.(14), the thickness of the plate is increased as shown in Fig.1(d). In the bridge axis direction, the section of Xu as shown in Fig.1(a) is reinforced. Table 1 shows the cross-sectional properties of the girder preliminary designed. In the table, the figures in the parenthesis are for the reinforced girder.

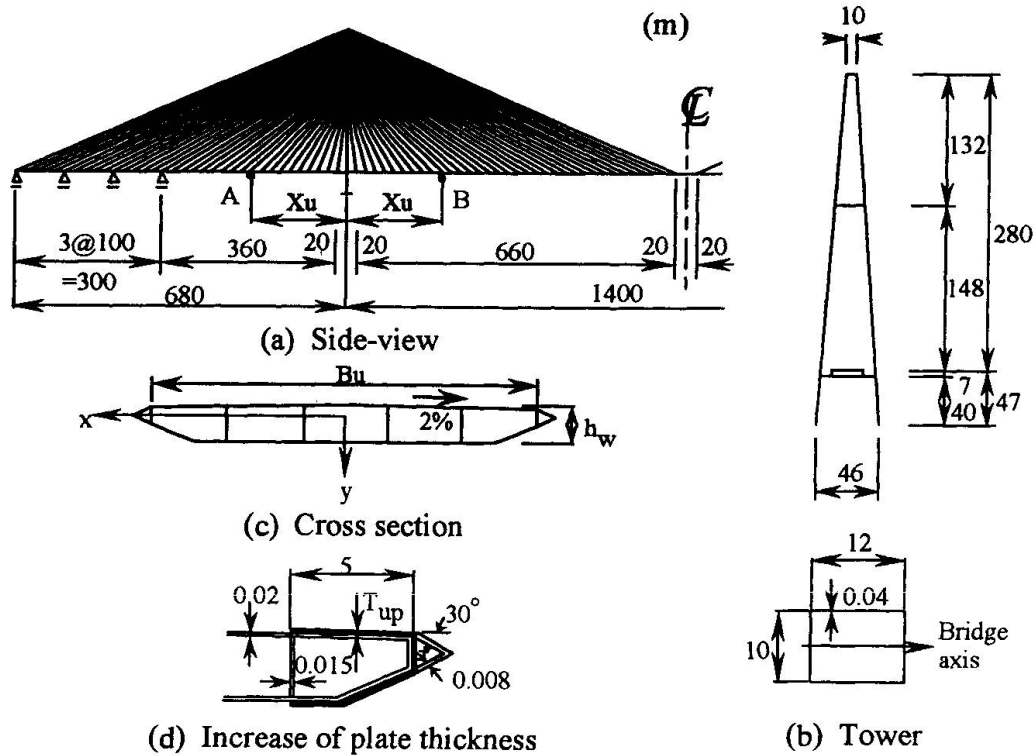


Figure 1: Bridge model

Table 1 : Cross sectional properties of the girder and tower

	Bu (m)	hw (m)	A (m ²)	I _x (m ⁴)	I _y (m ⁴)	J (m ⁴)	I _w (m ⁶)	W (tf/m)	X _u (m)
Girder	25	3.5	1.314 (2.243)	2.56 (4.050)	75.653 (177.323)	5.767 (9.395)	90.431 (314.397)	21.441 (28.871)	260
	25	4.0	1.348 (2.359)	3.291 (5.130)	76.932 (187.140)	7.133 (11.333)	106.659 (404.954)	21.815 (29.751)	200
	30	3.5	1.563 (2.134)	3.083 (3.987)	127.201 (222.835)	7.08 (9.615)	173.351 (369.716)	24.177 (28.871)	120
	30	4.0	1.605 (2.182)	4.002 (5.051)	129.658 (225.990)	8.889 (11.728)	210.045 (452.920)	24.639	140
Tower			1.76	30.667	40.32	39.273	—	19.342	—

4. RESULTS AND DISCUSSIONS

4.1 Load carrying capacity under in-plane load

Fig.2 shows incremental displacements of the bridge at ultimate state. In all cases, at points A and B, where the cross sectional properties are changed, the rapid increase of the vertical displacement is observed. In this region, the displacement in the bridge axis direction also increases rapidly. Hence, this is thought to be elasto-plastic global buckling of the girder. When in-plane instability occurs, the applied load of each model is from 2.75 to 2.90 times the dead load intensity. The large values are obtained. Since the effect of the local buckling of the stiffened plate is not taken into account in this analysis, it is predicted that the unstable behavior of the bridge models is controlled by the local buckling.

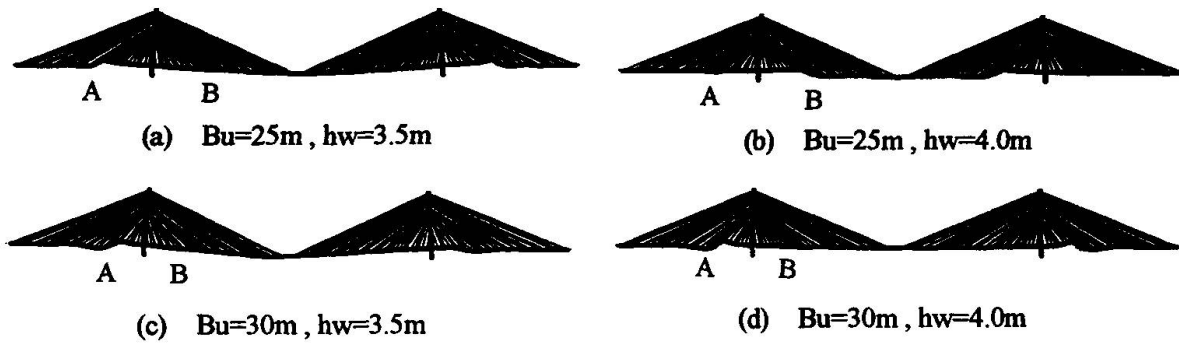


Figure2: Incremental displacement at ultimate state

4.2 Lateral torsional buckling instability under wind load

Fig.3 shows the lateral displacement, vertical displacement and rotational angle at the middle of the center span of the completed bridges. Fig.4 shows those at the tip of the cantilevered girder. In case of the completed bridges, at wind velocity of around 60m/s, nonlinear behavior of vertical displacement and rotational angle becomes prominent, and at the wind velocity from 77 to 80m/s, they diverges. This is lateral torsional buckling. In case of the bridge under construction, since the system is flexible, the larger lateral displacement is obtained. At the wind velocity of around 50m/s, nonlinear behavior of the vertical displacement becomes prominent and, at the wind velocity from 66 to 70m/s, the girder becomes unstable. The critical wind velocities calculated are enough high compared with the design wind velocities.

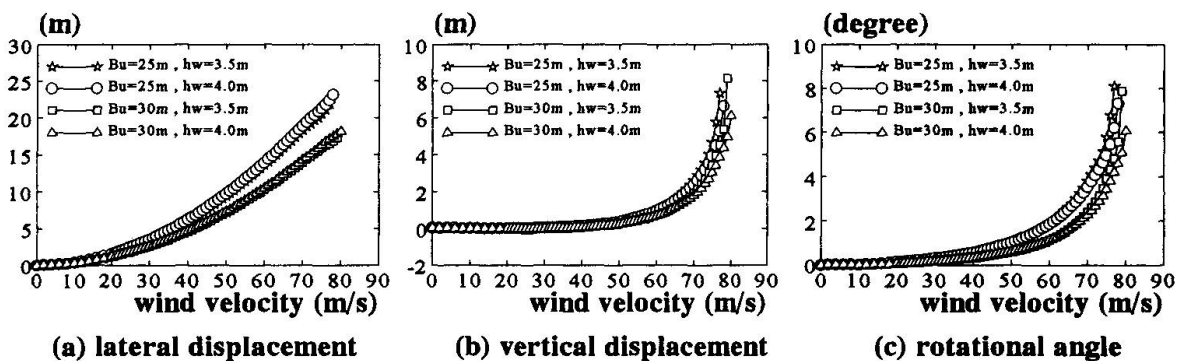


Figure3 : Displacement at the middle of the center span (after completion)

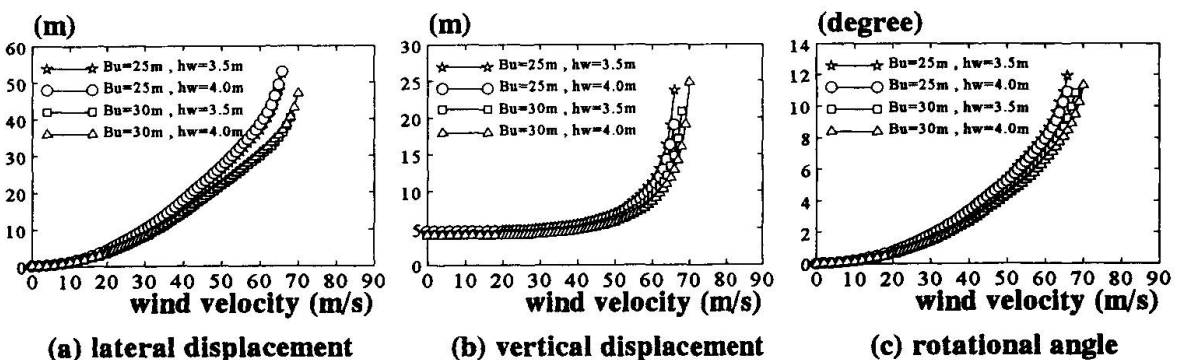


Figure4 : Displacement at the tip of the girder (under construction)



4.3 Flutter onset wind velocity

Table 2 shows the flutter onset wind velocity of the completed bridge and the bridge under construction, respectively. In the table, the figures in the parenthesis are wind velocities when the cable local vibration is taken into account. It is found that the flutter onset wind velocity is higher than the critical wind velocity under static wind load. It is also found that the effect of the cable local vibration on flutter onset wind velocity is prominent. From this result, it is concluded that the dimension of the girder is controlled by static instability.

Table2: Flutter onset wind verocity

Model	(m/s)	
	Completed [30-mode]	Under Construction [20-mode]
Bu=25m , hw=3.5m	120 (144)	100 (151)
Bu=25m , hw=4.0m	127	118
Bu=30m , hw=3.5m	120	102
Bu=30m , hw=4.0m	126 (151)	105 (168)

5. CONCLUDING REMARKS

We explained instability analyses of long-span cable-stayed bridges. The followings are main results obtained from this study.

- 1). In all cases, the factor of safety from 2.75 to 2.90 is obtained.
- 2). Flutter onset wind velocity exceeds 100 meters and is higher than the critical wind velocity of lateral torsional buckling under static load. It is found, among instability issues, that static instabilities under in-plane load and displacement-dependent wind load control the dimension of the girder.
- 3). On condition that the bridge is designed based on the procedure explained in Sec.3, the girder with the span/width ratio of around 60 and the span/depth ratio of around 400 can be used.

References

- 1) X.Xie, M.Nagai and H.Yamaguchi : Ultimate strength analysis and behavior of long-span cable-stayed bridges, Jour. of JSCE (in Japanese, under contribution)
- 2) X.Xie, H.Yamaguchi and M.Nagai : Static behaviors of self-anchored and partially earth-anchored long-span cable-stayed bridges, Int. Jour. of Structural Engineering and Mechanics, Vol.5, No.6, pp.767-774, 1997
- 3) V.Boonyapinyo, H.Yamada and T.Miyata : Nonlinear buckling instability analysis of long-span cable-stayed bridges under displacement-dependent wind load, Jour. of Structural Engineering, JSCE, Vol.39A, pp.923-936, 1993
- 4) M.Nagai, T.Ishida, X.Xie, H.Yamaguchi and Y.Fujino : Minimum girder width ensuring safety against static and dynamic instabilities of long-span cable-stayed bridges under wind load, Jour. of Structural Engineering, JSCE, 1998 (in Japanese, to appear)